Photodesorption and Photostability of Acetone Ices: Relevance to Solid Phase Astrochemistry

ARTICLE *in* THE JOURNAL OF PHYSICAL CHEMISTRY C · FEBRUARY 2014

Impact Factor: 4.77 · DOI: 10.1021/jp410745c

THE JOURNAL OF PHYSICAL CHEMISTRY C

Article

pubs.acs.org/JPCC

Photodesorption and Photostability of Acetone Ices: Relevance to Solid Phase Astrochemistry

Guilherme C. Almeida,*[,†] Sérgio Pilling,[‡] Diana P. P. Andrade,[‡] Nathany Lisbôa S. Castro,[†] Edgar Mendoza,[§] Heloísa M. Boechat-Roberty,[§] and Maria Luiza M. Rocco[†]

[†]Instituto de Química, Universidade Federal do Rio de Janeiro, 21941-909 Rio de Janeiro, RJ, Brazil

[‡]Instituto de Pesquisa e Desenvolvimento, Universidade do Vale do Paraíba, 12244-000 São José dos Campos, SP, Brazil

[§]Observatório do Valongo, Universidade Federal do Rio de Janeiro, 20080-090 Rio de Janeiro, RJ, Brazil

Supporting Information

ABSTRACT: Acetone, one of the most important molecules in organic chemistry, also a precursor of prebiotic species, was found in the interstellar medium associated with star-forming environments. The mechanisms proposed to explain the gas phase abundance of interstellar acetone are based on grain mantle chemistry. High energy photons coming from the stellar radiation field of the nearby stars interact with the ice mantles on dust grains leading to photoionization, photodissociation, and photodesorption processes. In this work we investigate the photodesorption and the photostability of pure acetone ices due to soft X-ray impact. Absolute desorption yields per photon impact for the main positive ionic fragments were determined at the O 1s resonance energy (531.4 eV). The photostability of acetone ice was studied by exposure to different irradiation doses with a white beam of synchrotron radiation. The degradation of the ice was monitored by NEXAFS around the O 1s threshold. From this study we determine the photodissociation cross-section to be about 1.5×10^{-17} cm^2 which allowed us to estimate the half-life for acetone ice in astrophysical environments where soft X-rays play an important role in chemical processes.

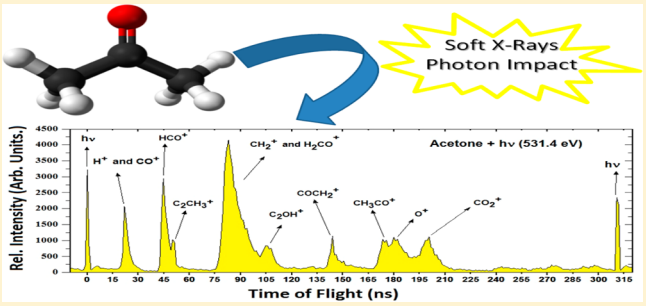

INTRODUCTION

Acetone ($CH_3-CO-CH_3$), one of the most important building blocks in organic chemistry, is largely used in many processes as solvent, and it is one of the most volatile organic compounds (VOC) in earth's troposphere.[1] Acetone was the first 10 atom molecule found in the interstellar medium (ISM),[2] first detected by Combes et al.[3] by the accurate measurement of acetone rotational lines at 82.9 and 112.4 GHz inside the Sgr B2 molecular cloud in a hot core known as the Large Molecule Heimat SgrB2 (N-LMH). Eighteen years later, acetone was confirmed toward the hot core of the Orion-KL star-forming region with the detection of more than 50 rotational transitions,[4] some of them belonging to the first vibrationally excited state. These astronomical data was of great importance for the efforts in understanding the formation mechanisms of interstellar acetone. The first mechanism proposed for the formation of interstellar acetone was a gas-phase radiative association between acetaldehyde (CH_3-CHO) and the CH_3^+ ion followed by dissociative recombination with an electron.[3,5] In 1990 Herbst et al.[6] showed that this radiative association mechanism was too slow to explain the high interstellar acetone abundances. Finally, Ehrenfreund and Charnley,[7] based on previous work of Millar et al.[8] on modeling the abundances of oxygen containing organic molecules in star-forming molecular clouds, showed that acetone formation on ISM gas requires grain mantle chemistry, where gas phase CO molecules condense on the surface of interstellar grains suffering hydrogen addition, leading to formyl radical (HCO) formation. The formyl radical rapidly suffers subsequent H, C, O, N atom additions, leading to complex organic molecules, like isocyanic acid (HNCO), ketene (H_2C_2O), formaldhyde (H_2CO), methanol (CH_3OH), ethanol (CH_3CH_2OH), and acetaldhyde (CH_3CHO). Further, methanol and acetaldehyde react, leading to acetone, but it is not clear if this step occurs in the ice phase or in the gas phase as the grain mantles are evaporated. In order to quantify the role of acetone and to understand the chemical evolution of complex organic molecules in icy mantles of dust grains, and in the gas phase it is necessary to establish the main formation paths, which requires a detailed study of the processes of excitation, ionization, dissociation, and desorption of these molecules caused by the interaction with ionizing agents, like UV, X-ray photons, and charged particles such as electrons and protons.

Inner-shell excitation of gas phase acetone received great attention during the past decades, mostly because acetone is a

Received: October 31, 2013
Revised: February 25, 2014

   dx.doi.org/10.1021/jp410745c | J. Phys. Chem. C XXXX, XXX, XXX−XXX

relative small system with two distinct nonequivalent organic groups, i.e., the methyl groups (CH_3) and the carbonyl group (CO). The first K-shell spectra of acetone were reported by Wight and Brion[9] at the carbon K-edge and later by Hitchcock and Brion[10] at the carbon and oxygen K-edges, using inner-shell electron energy-loss spectroscopy (ISEELS). Peak assignments were performed by comparison with ISEELS spectra of methane and formaldehyde.[10,11] Core excitation thresholds for carbon and oxygen were experimentally determined by X-ray photoelectron spectroscopy (XPS) by Jolly and Schaaf,[12] for a series of carbonyl containing compounds. Using the XPS technique with an Al Kα radiation source together with theoretical calculations, Correia et al.[13] found out the ionization thresholds for C_{CH3}1s, C_{CO} 1s, and O 1s showing that the C_{CO} 1s electrons are more tightly bound than the C_{CH3} 1s electrons. The development of monochromatic synchrotron radiation allowed the acquisition of high resolution inner-shell spectra of organic molecules and so a huge number of works investigating the K-shell spectra of functional organic molecules appeared in the literature. For acetone, we can mention the work of Sham et al.[14] and Thompson et al.[15] The first group measured the near-edge X-ray absorption fine structure (NEXAFS) spectra of acetone at the oxygen and carbon K-edges and the second measured the resonant auger spectra (RAS) also at the C and O K-edges. These data together with quantum chemical theoretical calculations[16] not only confirmed the prior peak assignments performed by ISEELS and XPS, but also helped on the understanding of the structure of the 1s $\rightarrow \pi^*$ resonances, the Rydberg states and the proper set up of the ionization thresholds and the σ^* shape resonances above it.

Photofragmentation of gaseous acetone due to inner-shell excitation at the carbon and oxygen K-edges has been investigated by several authors[17−19] with the aid of time-of-flight mass spectrometry (TOF-MS) and monochromatic synchrotron radiation. These studies showed that H^+ and CH_3^+ fragment ions have the highest yields near the C 1s and O 1s edges and that the ionization around the C 1s energy favors the C−C bond rupture, enhancing the yield of CH_n^+ type ions, while the ionization around O 1s energy favors the loosening of the C═O bond, enhancing the yield of $C_2H_n^+$ and $C_3H_n^+$, n = 0−3, type ions. Suzuki and Saito[20] investigated the ion pair formation with the photoion−-photoion (PIPICO) coincidence technique and found no site-selective reaction pathways for ion-pair formation at the C 1s and O 1s edges. They also found that the yield of the ion-pair groups of H^+-$C_nH_m^+$ type decreases with the increasing of the number of hydrogen atoms.

Valence shell excitation and ionization of gas phase acetone with UV photons have been extensively studied due to its importance to atmospheric photochemistry. We will limit our discussion to some astrochemical relevant work. Koch et al.[21] determined the UV absorption cross sections for the n $\rightarrow \pi^*$ system at temperatures between 300 and 1100 K and found that the strength of the system grows with the temperature due to the vibrationally excited states causing a shift to higher energies in the UV spectra. Fogleman et al.[22] studied the vacuum ultraviolet (VUV) dissociative photoionization onsets for the production of acetyl ion $(CH_3CO)^+$ by measuring the threshold photoelectron-photoion coincidence (TPEPICO) mass spectra as a function of the ion internal energy and determined the heat of formation for this ion and its radical $(CH_3CO)^{\bullet}$. Rennie and co-workers[23] acquired the valence shell, the threshold photoelectron spectrum and the TPEPICO mass spectra using monochromatic synchrotron radiation. They found that the $(CH_3CO)^+$ ion completely dominates the mass spectrum for energies below 15 eV and above this energy fragments like CH_3^+, $C_2H_3^+$, $C_2H_2^{+\bullet}$, $CH_2CO^{+\bullet}$, and $CH_2^{+\bullet}$ appear on the spectrum.

Ice phase acetone was not so well investigated as gas phase, but there are some studies with acetone molecules condensed on solid Ar and metallic substrates. These studies are relevant to ice phase astrochemistry, since, as mentioned above, acetone is believed to be formed in the ice mantles of interstellar grains. Lepage and co-workers[24,25] studied condensed films of acetone on solid Ar and on Pt(111) with low energy electron energy loss spectroscopy (EELS). They reported the production of CO fragments, which remain trapped within the bulk of acetone ice. They also investigate the valence shell electronic spectra and the vibrational spectra by this technique and discussed the main differences between these spectra and the spectra acquired in the gas phase. Kusunoki and co-workers[26] studied the thermal and nonthermal desorption of acetone condensed on a Si(100) substrate cooled at 95 K by temperature programmed desorption (TPD) and by irradiation with a 193 nm pulsed laser. They could determine the desorption energy for ice phase acetone and found that thermal desorption does not produce dissociation products while nonthermal desorption with UV pulsed laser produces CH_3, CO and CH_3CO fragments different from the gas phase dissociation that only produces CO and CH_3 fragments.[27] Sekiguchi et al.[28] employed photon stimulated ion desorption (PSID) at the carbon K-edge of condensed acetone on Si(100) substrate cooled at 93 K. By varying the film thickness, they found that small fragments like H^+ and CH_n^+ dominates the PSID mass spectra in thin films due to the interaction with the substrate, but when the thickness of acetone films grows the desorption yield of fragments like $C_2H_n^+$, $C_3H_n^+$, CH_3O^+, CH_3CO^+, and the protonated cluster $(CH3)_2COH^+$ became comparable with those of the small fragments.

The study of molecular clusters was relevant for the understanding of ice phase behavior of acetone. The photoionization of $(CH_3COCH_3)_n$, n = 1−4, was studied by Trott et al.[29] In this study, they measured the ionization energies for this series of clusters and found a linear decreasing relationship of $1/n$. The authors also measured the ion yield curves for this series of clusters and reported the production of CH_3CO^+ and $(CH_3COCH_3)\cdot CH_3CO^+$ fragments by ultraviolet photoionization of these clusters. Tamenori et al.[30] investigated hydrogen bonding on acetone clusters by NEXAFS, density functional theory (DFT) calculations and partial-ion-yield (PIY) method at the carbon and oxygen K-edges. They found slightly differences in the C1s and O1s photoabsorption spectra of the clusters in relation to the single molecule. DFT calculations showed that these differences were mainly due to the nature of the hydrogen bonding interactions. Matsuda et al.[31] and Guan et al.[32] studied the photoionization of acetone and its clusters by UV and infrared double resonance spectroscopy. This technique was important for the elucidation of the intermolecular interactions between the carbonyl and methyl groups and to elucidate the structural conformation of acetone clusters.

In the present work we employed the PSID technique by the impact of soft X-ray photons at the oxygen K-edge and studied the photostability of acetone ices due to exposure to different soft X-rays doses of a white beam of synchrotron radiation (SR). Absolute ionic yields for the fragments desorbed,

dx.doi.org/10.1021/jp410745c | J. Phys. Chem. C XXXX, XXX, XXX−XXX

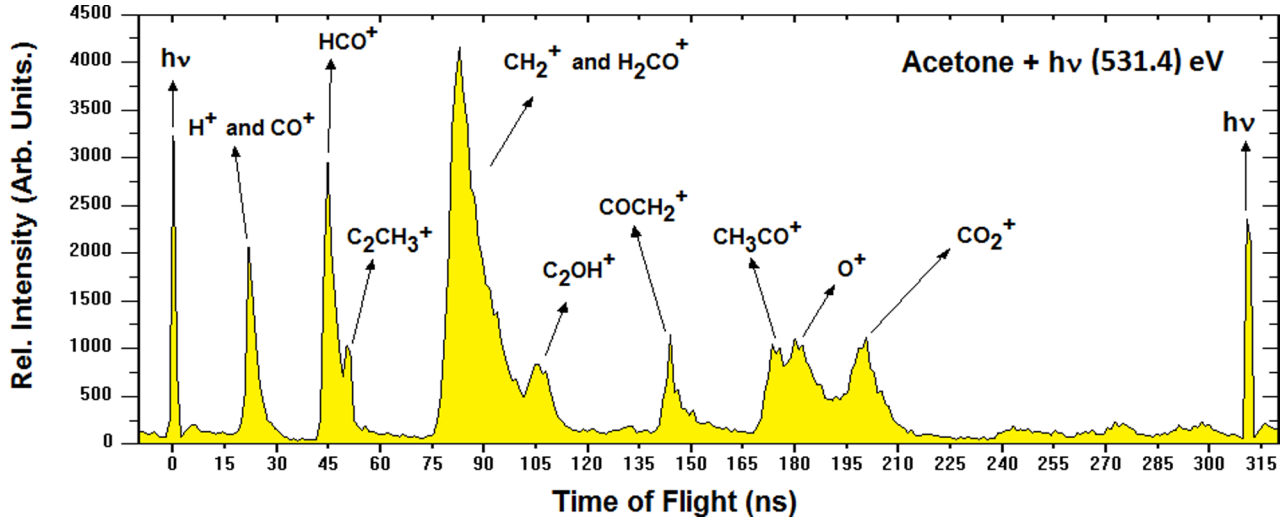

Figure 1. Positive PSID spectra of ice phase acetone at 531.4 eV photon energy.

photodissociation cross sections and the half-life for ice phase acetone were determined. The results were interpreted in terms of astrophysical implications.

EXPERIMENTAL SETUP

All experiments were carried out at the Brazilian Synchrotron Light Source (LNLS) at the Spherical Grating Monochromator (SGM) beamline. The experimental setup consists of a *X,Y,Z* sample manipulator, a TOF-MS spectrometer, a helium cryostat and a sample injection system housed in an ultrahigh vacuum chamber (UHV) with a base pressure of about 10^{-9} Torr. Acetone was condensed onto a very thin gold foil cooled to 10 K inside the previous evacuated UHV chamber. The condensed sample was placed at 45° with respect to the incident SR beam. A thermocouple was used to determine the icy sample temperature during the measurements. Acetone was purchased from Synth Services Inc. with more than 99% of purity.

Photon Stimulated Ion Desorption (PSID) Studies. The acetone ice was irradiated with monochromatic SR beam at 531.4 eV photon energy. During this experiment the electron storage ring was operating in the single-bunch (SB) mode with a period of 310.88 ns, pulse width of 60 ps, and a photonic incidence of 1550 photons per bunch. The experimental setup for the PSID experiments is described in detail in Rocco et al.,[33] so only a brief explanation will be given here. Desorbed ions were collected and mass/charge analyzed by the TOF-MS. This spectrometer basically consists of an electrostatic ion extraction system, a drift tube and a pair of microchannel plate (MCP) detectors, disposed in the chevron configuration. The output signal of the detector was processed by a standard pulse counting system and used to provide the stop signal to the time-to-digital converter (TDC). The potentials were chosen after ion optic simulations carried out using the SIMION 3D 7.0 program. A 1/148 divider was used to take the SR pulse timing from the 476.066 MHz frequency signal from the microwave cavity of the storage ring, which was used to trigger the experiment and to give the start signal for the TDC.[34] Simulations were carried out using the SIMION 3D 7.0 program in order to obtain the experimental time-of-flight (TOF) of the desorbed ions. The ionic trajectories simulations were performed taking into account that ions could desorb within a kinetic energy spread of 0−15 eV and at angles between −90° and +90°. In the SB mode, the spectra are taken in the time window of 310.88 ns, so the position of each ion in this time window should be determined by the ratio TOF/310.88. The integer part of this quotient corresponds to the number of SR cycles, and the fractional component defines the position of each ion peak within the time window as shown in the equation below:

$$\mathrm{TOF(SB)} = ([\mathrm{TOF(Simion3D)}/310.88] - n)310.88 \quad (1)$$

where [TOF(SB)] is the time-of-flight of the ions observed in the spectra taken in the 310.88 ns time window, [TOF(Simion 3D)] is the experimental time-of-flight obtained by simulating the ion trajectories within the experimental conditions, and *n* is the number of SR cycles which corresponds to the fractional part of the [TOF(Simion3D)/310.88] ratio.

Photostability Studies. The acetone ice was exposed to different soft X-ray doses (0 to 200 min), provided by a white beam of SR (∼0.01−2000 eV). In this experiment the storage ring was operated in the multibunch (MB) mode, with 148 equal electron packets of 60 ps width and 2.1 ns of spacing between them. In the MB mode the spacing between the packets are shorter than the response time of the measuring instruments, so if the storage ring is being operated at this mode we can consider that the synchrotron light is essentially continuous from our perspective. In situ analysis was performed by NEXAFS at the O K-edge. NEXAFS spectra were recorded by measuring the drain current at the sample, the well-known total electron yield (TEY) regime. The final data was normalized by the storage ring current in order to correct for eventual fluctuations in the beam intensity. The energy calibration was performed by taking the value for the O 1s → π^* resonance from the gas phase core excitation database,[35] and this resonance peak was used for monitoring the degradation of the ice after each soft X-ray dose.

RESULTS AND DISCUSSION

The PSID spectrum for positive desorbed fragments from acetone ice at 531.4 eV photon energy is shown in Figure 1. The two sharp peaks at the extremes of the spectrum are due to scattered photons, occurring every 310.88 ns and coinciding with the signal from the microwave cavity of the storage ring.

dx.doi.org/10.1021/jp410745c | J. Phys. Chem. C XXXX, XXX, XXX−XXX

The spectrum, as expected for O1s threshold, shows high degree of fragmentation of the acetone molecule. In contrast with valence shell photoionization,[23] no parent molecular ion was observed and the acetyl ion, CH_3CO^+, m/z = 43, does not dominate the mass spectrum as the main produced fragment, having comparable intensity with smaller fragments like H^+, CH_2^+, O^+, and HCO^+, as observed in other inner-shell photoionization studies in the gas phase,[17−19] in the ice phase[28] and cluster beams.[30] The production of CH_n^+, $C_2H_n^+$, and $C_3H_n^+$ series of positive fragments were reported in the ice phase carbon K-edge photoionization spectra.[28] No such series of fragments were observed in the 531.4 eV PSID spectrum.

From the simulations we found that the first peak in the spectra could be related to H^+ and CO^+ fragments and that the broad peak between 75 and 100 ns to CH_2^+ and H_2CO^+ fragments. We have performed the deconvolution of these peaks by fitting Gaussians in order to determine the area of each fragment peak, as shown in Figure 2. From that we found

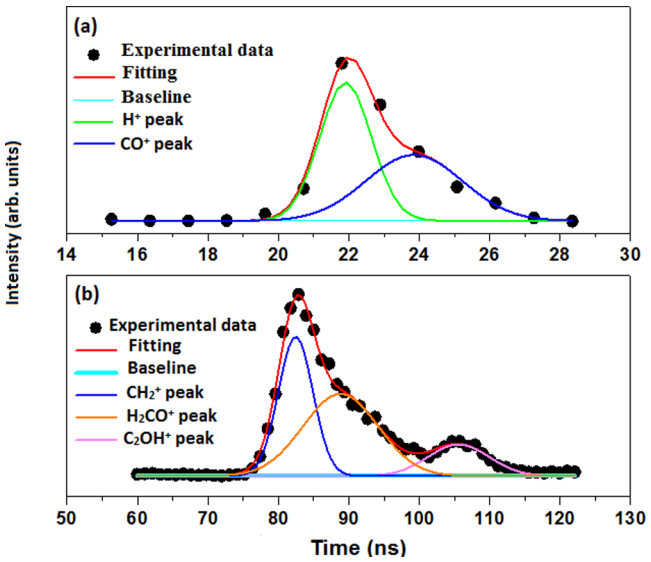

Figure 2. Deconvolution of the peaks at 531.4 eV photon energy from the positive PSID spectrum. (a) Deconvolution of the H^+/CO^+ peaks; (b) deconvolution of $CH_2^+/H_2CO^+/C_2OH^+$ peaks.

that H^+ falls at 21 ns, CO^+ at 24 ns, CH_2^+ at 83 ns, and H_2CO^+ at 89 ns with respect to the 310.88 ns time-window of the PSID spectra. In Figure 2a, the first Gaussian fit corresponds to H^+ signal and the second to CO^+ signal, which gives 53% of the total area corresponding to the H^+ fragment and the others 47% to the CO^+ fragment. In Figure 2b, the first Gaussian fit corresponds to CH_2^+ signal, the second one to the H_2CO^+ signal and the third one to the C_2OH^+ signal, which gives 37% of the total area corresponding to the CH_2^+ fragment, 48% of the total area corresponding to the H_2CO^+ fragment and the others 15% to the C_2OH^+ fragment. This was taken in consideration to calculate the photodesorption yields for these fragments. The fragment m/z = 14 was signed as CH_2^+ but could also be the CO^{+2} fragment. Since double ionized fragments have low probability to desorb, we believe that this peak is mainly due to the CH_2^+ fragment.

In order to determine the absolute photodesorption yield values, Y_p (ions/photon), presented in Table 1, we employed the following procedure. First we determined the area (A) of each peak and divided this value by the number of bunches

Table 1. Desorption Yield, Y_p (Ions/Photon), of Fragments Desorbed from Icy Acetone at 10 K Due to Soft X-ray Photons at 531.4 eV

m/z	ion	Y_p ($\times 10^{-8}$) ions/photon
1	H^+	0.06
14	CH_2^+	0.97
16	O^+	0.36
28	CO^+	0.05
29	HCO^+ or $C_2H_5^+$	0.32
30	H_2CO^+	1.26
39	$C_2CH_3^+$	0.12
41	C_2OH^+	0.39
42	CH_2CO^+	0.34
43	CH_3CO^+	0.26
44	CO_2^+	0.72

(N_b) and the number of photons per bunch (n_{ph}), as shown in eq 2. On the single-bunch mode, the number of incident photons on a 2 mm^2 surface during 60 ps (pulse duration) is about 1550 photons $bunch^{-1}$, which corresponds to a photon flux of 5×10^{11} photons s^{-1} cm^{-2}.

$$Y_p = \frac{A}{N_b n_{ph}} \quad (2)$$

The desorbed fragments from icy acetone and their photodesorption yields derived from eq 2 are shown in Table 1. CH_2^+, H_2CO^+, and CO_2^+ were the main desorbed fragments. Carbon dioxide is believed to be formed by fragment recombination following the pathways below.[36]

$$CO^+ + CO \rightarrow CO_2^+ + C \quad (3)$$

$$CO + O^+ \rightarrow CO_2^+ \quad (4)$$

These pathways explain the low desorption yields observed for CO^+ and O^+ when compared with CO_2^+. Gas phase studies at the C1s and O1s threshold[20] showed that core excitation tends to favor the C−H bond rupture leading to fragments with less hydrogen atoms. This effect can explain the desorption of fragments like C_2OH^+ and $C_2CH_3^+$ and the higher yields of CH_2^+ fragment instead of CH_3^+. X-ray induced ion desorption from condensed systems can occur by direct or indirect processes.[37] In the direct process, the inner-shell excitation will produce core holes, and since acetone is composed of light elements, the relaxation process will proceed preferentially via the Auger mechanism,[38] which produces positive holes in valence orbitals causing the direct desorption of fragments due to strong Coulombic repulsion. In the indirect process, the desorption of fragments is caused by valence excitations and ionizations induced by secondary electrons which are mainly Auger electrons and photoelectrons originated in the bulk of the ice.[39]

Taking into consideration that the direct and indirect desorption processes can occur, and previous PEPICO and PIPICO gas phase studies at the O1s and valence threshold,[18,20,23] we suggest some fragment formation routes:

$$(CH_3)_2CO^{+2} \rightarrow CH_2^+ + H^+ + CH_3CO + H \quad (5)$$

$$CH_3COCH_3^+ \rightarrow CH_3CO^+ + CH_3\cdot \quad (6)$$

$$CH_3COCH_3^+ \rightarrow CH_2CO^+ + CH_4 \quad (7)$$

dx.doi.org/10.1021/jp410745c | J. Phys. Chem. C XXXX, XXX, XXX−XXX

Formaldehyde ion (H_2CO^+) and formyl radical (HCO^+) were not observed in previous gas phase[17−20] and cluster photoionization[30] studies of acetone at the C and O K-edges. We believe that these fragments are being formed by hydrogen addition to the CO molecule as suggested by Ehrenfreund and Charnley[7] on their model for formation of large organic molecules in star-forming regions. Hydrogen ions and radicals could be produced by the fragmentation pattern shown in reaction 5, which also produces the CH_2^+ fragment. From Table 1 we can observe that there is a great difference between the desorption yields of H^+ and CH_2^+ fragments which suggests that part of the hydrogen ions are reacting with other fragments before desorbing from the ice. HCO^+ and H_2CO^+ fragments were not observed in inner-shell excitation of condensed acetone at the C K-edge,[28] but the photoionization studies of acetone molecular clusters[30] showed that excitation at the O K-edge can favor the desorption of oxygen type fragments.

Reactions 6 and 7 have close activation energy, but at temperatures close to 0 K the methane loss, reaction 7, is favored.[23] This can explain the fact that the ketene ion (CH_2CO^+) yield is higher than that for the acetyl ion (CH_3CO^+). The absence of CH_3^+ ion in the PSID spectrum suggests that methyl fragment is desorbing as a neutral fragment; one possible formation route for neutral CH_3 is shown in reaction 6. Similar behavior was observed for the OH fragment in PSID and ESID spectrum of methanol.[40,41] The production of neutral CH_3 fragment was also reported on the photoionization of clusters of $(CH_3COCH_3)_2$[29,32] type. In the PSID spectrum of methanol high yields were also observed for CH_2^+ and H_2CO^+ fragments.

The fragmentation pattern observed in the condensed acetone spectrum strongly suggests that if acetone is frozen on dust grains, it can act as a source of carbon monoxide, carbon dioxide, methane, formaldehyde and hydrogen radicals to the gas phase environment of interstellar medium. In order to estimate the photostability of ice phase acetone in the ISM we have employed a white beam of SR, measuring the degradation of acetone ice with time exposure. The integrated photon flux at this energy range was 1.7×10^{13} photons s^{-1} cm^{-2}. NEXAFS spectrum at the oxygen K-edge of acetone ice before irradiation is shown in Figure 3. No significant differences from the gas phase photoabsorption spectra[35] were observed. Tamenori et al.[30] observed a shift of 0.13 eV to higher energy at the O1s → π* resonance peak in the acetone cluster NEXAFS spectrum as compared to the single molecule spectrum. Theoretical calculations performed by the authors showed that this shift is due to hydrogen-bonding interactions. Ice phase strongly favors hydrogen bonding in molecular compounds like acetone, and for this reason we would expect to observe a similar shift in our ice phase spectrum, but the energy resolution of the SGM beamline of 0.2 eV limited us to performing such investigation. Peak assignments were performed based on the work of Sham et al.[14] and Hitchcock and Brion.[10] We use the O1s → π* resonance peak to perform the monitoring of the ice degradation within the time doses of white beam irradiation.

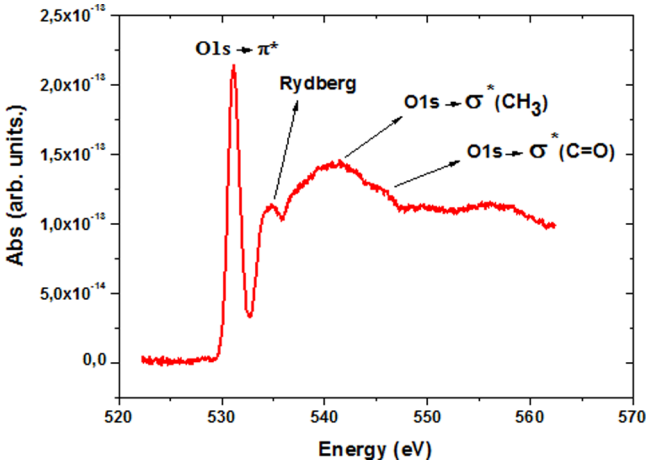

Figure 3. O 1s NEXAFS spectrum for 10 K acetone ice before irradiation.

Assuming that the ice is optically thin and the flux of irradiation at the sample is constant, we can assume a first order decay for the ice photolysis and derive the photodissociation rate,[42,43] which is the product of the destruction cross section (σ_d) and the photon fluence (ϕ) at the sample. The photon fluence is derived by the product between the photon flux at the sample and the irradiation time in seconds. Figure 4 shows the evolution of the O1s → π* peak area against irradiation time doses.

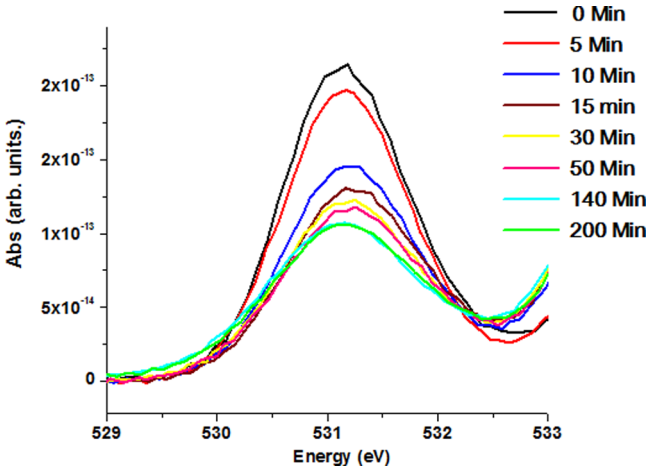

Figure 4. Evolution of degradation of acetone ice due to white beam exposure, following the O1s → π* resonance probed by NEXAFS.

After a certain irradiation time, we can observe a broadening followed by a downward shift of the O1s → π* resonance that became more prominent after long time exposure. Similar spectral changes were reported on the irradiation of methanol ices by Hudson and Moore[44] and in an X-ray irradiation damage study on alkanethiolates monolayers deposited on a gold substrate by Heister et al.[45] These authors attribute these spectral changes to the loss of homogeneity of the surface, which is an effect of the chemical enrichment of the surface composition by the photoproducts. The PSID experiments showed that soft X-ray impact on acetone ice can produce CO, CO_2, CH_4, H_2CO, and hydrogen radicals that could easily react leading to H_2. Due to the low temperature of the ice in our experiments, 10 K, some amount of these compounds, together with any other photoproduct produced by a recombination reaction between ions, radicals and free electrons could be retained in the ice matrix, causing the loss of the degree of homogeneity of acetone molecules in the ice matrix.

It is important to note that the degradation rate is falling, as expected for a first order decay behavior; however, after 140

dx.doi.org/10.1021/jp410745c | J. Phys. Chem. C XXXX, XXX, XXX−XXX

min of irradiation, a nonfirst-order behavior takes place, and no more significant decay is observed. The nonfirst-order behavior after a certain time of irradiation can be explained by the production of photoproducts that can react producing the initial compound again or other compounds, as the ones mentioned above, that enhance the absorption of the photon flux causing the decrease of photolysis efficiency and ice bulk coverage protection for further photolysis.[42,46]

Taking into consideration the behavior observed in the acetone ice degradation, we applied the kinetic model described in eq 8 in order to derive the photodissociation rate. The integrated area of the O1s → π^* resonance peak as a function of time can be modeled by eq 8.

$$A(t) = A_o e^{-\sigma_d \Phi(t)} + A_b \quad (8)$$

where A_o is the integrated peak area of the ice surface before irradiation starts ($t = 0$), $\Phi(t)$ is the photon fluence in photons cm^2 at a given time t, σ_d is the photodissociation cross section considering the effects of soft X-ray photons coming from the white beam of SR, and A_b is the integrated peak area for the ice bulk or unirradiated ice. A_b can be considered as the terminal integrated area of the O1s → π^* resonance peak after long time of exposure.

Figure 5 shows the fitting of this equation to the experimental data acquired with the medium value for the

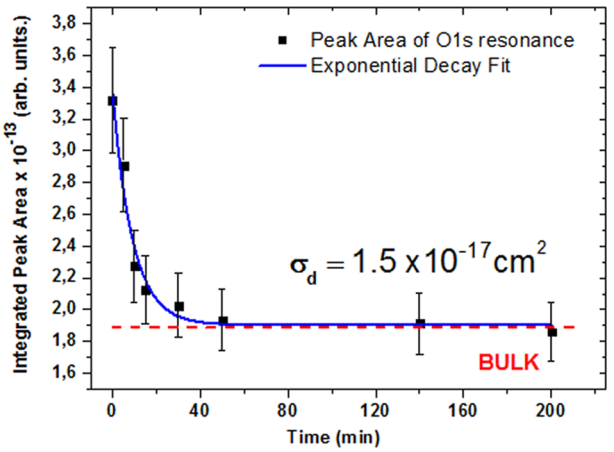

Figure 5. Area of the O1s → π^* resonance peak as a function of the time of exposure and the fitting of the experimental data with eq 8

soft X-ray destruction cross section derived. We found a value of 1.904×10^{-13} for A_b. This value differs 0.4% from the value found for $A_{(140min)}$ and 3% from the value found for $A_{(200min)}$, so we assume that the standard error for the calculated peak areas is 3%. The determined value for the destruction cross section employing SR white beam photons was 1.5×10^{-17} cm^2.

Once the destruction cross section and the photon flux are known we can estimate the half-life for ice phase acetone and extrapolate the observed behavior to astrophysical environments where soft X-ray photon flux coming from the nearby stars plays an important role in the evolution of the interstellar chemistry. The half-life for the acetone molecule can be estimated as given by eq 9.[42,47]

$$t_{1/2} = \frac{\ln 2}{\sigma_d \varphi} \quad (9)$$

where φ is the photon flux (photons s^{-1} cm^{-2}) of a known astronomical object. Space telescopes like ROSAT and Chandra have measured strong X-ray fluxes coming from young stellar objects (YSOs). These X-ray fluxes are 3 orders of magnitude higher for premain sequence stars than for main sequence stars[48] like our sun. T-Tauri stars are a class of premain sequence stars, found near molecular clouds, in the process of contraction to the main sequence. Kastner et al.[49] showed that T-Tauri stars with accreting disks, which are a rotating disk of gas and dust that surrounds the protostar, where a planetary system will be further developed,[40] have high soft X-ray emissions. The origin of these strong soft X-ray emissions are still object of intense study, but it is believed that it is due to strong magnetic interactions between the stellar object and its circumstellar accretion disk.[50] TW Hya is the closest, 56 pc, T-Tauri star to our solar system, and it has a massive accreting disk, so we can consider this star as the main source of soft X-rays in the limits of our solar system, where soft X-rays flux coming from the sun and other solar system bodies is insignificant and grain mantle chemistry plays an important role, being in constant evolution. We can use the integrated soft X-ray photon flux coming from TW-Hya to estimate the half-life of grain mantle acetone in the Oort cloud. Kastner et al.[49] derived from Chandra data an integrated soft X-ray flux of 2.5×10^{-3} photons s^{-1} cm^{-2} coming from TW-Hya. Stelzer and Schmitt[50] found a similar value from XMM-Newton satellite data.

We found an estimated half-life for icy acetone in outer Oort cloud of 5.87×10^{11} years. This means that acetone survives in ice phase for a long period in the limits of our solar system and will participate actively on the development of ice chemistry complexity. If we consider other cold parts of the ISM, like dense molecular clouds,[43] where soft X-ray fluxes are high enough, our experiment showed that ice phase acetone can be effectively destructed. The SGM beamline has an estimated photon flux of $\sim 1.7 \times 10^{13}$ photons s^{-1} cm^{-2} at white beam mode, meaning that on these conditions the half-life of acetone ice is just 47 min.

CONCLUSIONS

In a contribution on experimental investigation of molecules of astrophysical interest, we studied the soft X-ray photon impact on ice acetone. From the photon stimulated ion desorption experiments at the O 1s absorption edge we obtained absolute desorption yields per photon impact for the identified positive fragments. H_2CO^+, CH_2^+, and CO_2^+ were the most abundant fragments. The fragment formation pathways give an idea of frozen acetone behavior in interstellar space. From the ice photostability studies monitored by NEXAFS spectroscopy we determined a value of 1.5×10^{-17} cm^2 for the destruction cross section employing soft X-ray photons. This value allowed us to estimate the half-life of ice phase acetone molecules and extrapolate this behavior to astrophysical environments where soft X-rays play an important role on the development of interstellar chemistry complexity.

ASSOCIATED CONTENT

Supporting Information

Table comparing the time-of-flight (TOF) values obtained from the simulations with the SIMION 3D 7.0 software, the TOF (SB) values for the 310.88 ns time window spectrum calculated with eq 1, the number of SR cycles (n), and the TOF

dx.doi.org/10.1021/jp410745c | J. Phys. Chem. C XXXX, XXX, XXX−XXX

(SB) observed in the spectrum. This material is available free of charge via the Internet at http://pubs.acs.org.

AUTHOR INFORMATION

Corresponding Author

*E-mail: luiza@iq.ufrj.br.

Notes

The authors declare no competing financial interest.

ACKNOWLEDGMENTS

The authors acknowledge Conselho Nacional de Desenvolvimento Científico e Tecnológico (CNPq), Coordenação de Aperfeiçoamento de Pessoal de Nível Superior (CAPES), and Fundação de Amparo à Pesquisa do Estado do Rio de Janeiro (FAPERJ) for financial support and Prof. Raul Baragiola, University of Virginia, and Dr. Michel Nuevo, NASA Ames Research Center, for helpful discussions on the photostability results.

REFERENCES

(1) Harrison, J. J.; Allen, N. D. C.; Waterfall, A. M.; Bernath, P. M.; Remedios, J. J. Mid-Infrared Absorption Cross Sections for Acetone (Propanone). *J. Quant. Spectrosc. Radiat. Transfer* **2011**, *112*, 457−464.

(2) Snyder, L. E.; Lovas, F. J.; Mehringer, D. M.; Miao, N. Y.; Kuan, Y. J.; Hollis, J. M.; Jewell, P. R. Confirmation of Interstellar Acetone. *Astrophys. J.* **2002**, *578*, 245−255.

(3) Combes, F.; Gerin, M.; Wootten, A.; Wlodarczak, G.; Clausset, F.; Encrenaz, P. J. Acetone in Interstellar Space. *Astron. Astrophys.* **1987**, *180*, L13−L16.

(4) Friedel, D. N.; Snyder, L. E.; Remijan, A. J.; Turner, B. E. Detection Of Interstellar Acetone Toward The Orion-KL Hot Core. *Astrophys. J.* **2005**, *632*, L95−L98.

(5) Groner, P. Acetone: Laboratory Assignments and Predictions Through 620 GHZ for the Vibrational-Torsional Ground State. *Astrophys. J. Suppl. Ser.* **2002**, *142*, 145−151.

(6) Herbst, E.; Giles, K.; Smith, D. Is Interstellar Acetone Produced By Ion−Molecule Chemistry? *Astrophys. J.* **1990**, *358*, 468−472.

(7) Ehrenfreud, P.; Charnley, S. B. Organic Molecules in the Interstellar Medium, Comets and Meteorites: A Voyage from Dark Clouds to the Early Earth. *Annu. Rev. Astron. Astrophys.* **2000**, *38*, 427−483.

(8) Millar, T. J.; Herbst, E.; Charnley, S. B. The Formation of Oxygen-Containing Organic Molecules In The Orion Compact Ridge. *Astrophys. J.* **1991**, *369*, 147−156.

(9) Wight, G. R.; Brion, C. E. Carbon K-Shell Excitation in Acetone by 2.5 keV Electron Impact. *J. Electron Spectrosc. Relat. Phenom.* **1974**, *4*, 347−350.

(10) Hitchcock, A. P.; Brion, C. E. Inner-shell Excitation of Formaldehyde, Acetaldehyde and Acetone Studied by Electron Impact. *J. Electron Spectrosc. Relat. Phenom.* **1980**, *19*, 231−250.

(11) Wight, G. R.; Brion, C. E. K-shell Excitation of CH_4, NH_3, H_2O, CH_3OH, CH_3OCH_3 and CH_3NH_2 by 2.5 keV Electron Impact. *J. Electron Spectrosc. Relat. Phenom.* **1974**, *4*, 25−42.

(12) Jolly, W. L.; Schaaf, T. F. π-Donor Relaxation in the Oxygen 1s Ionization of Carbonyl Compounds. *J. Am. Chem. Soc.* **1976**, *98*, 3178−3181.

(13) Correia, N.; Brito, A. N.; Keane, M. P.; Karlsson, L.; Svensson, S.; Liegener, C. M.; Cesar, A.; Agren, H. Doubly Charged Valence States of Formaldehyde, Acetaldehyde, Acetone, and Formamide Studied by Means of Photon Excited Auger Electron Spectroscopy and Ab Initio Calculations. *J. Chem. Phys.* **1991**, *95*, 5187−5197.

(14) Sham, T. K.; Yang, B. X.; Kirz, J.; Tse, J. S. K-edge Near-edge X-Ray-Absorption Fine Structure of Oxygen- and Carbon-Containing Molecules in the Gas Phase. *Phys. Rev. A* **1989**, *40*, 652−669.

(15) Thompson, D. B.; Ji, D.; Lee, K.; Ma, C. I.; Hanson, D. M. Excitation and Decay Spectra of Core-Excited Resonances in Acetone. *J. Phys. B: At. Mol. Opt. Phys.* **1999**, *32*, 2649−2666.

(16) Yang, B. X.; Agren, H.; Carravetta, V.; Pettersson, L. G. M. Static Exchange and Quantum Defect Analysis of X-ray Absorption Spectra of Carbonyl Compounds. *Phys. Scr.* **1996**, *54*, 614−624.

(17) Eberhardt, W.; Sham, T. K.; Carr, R.; Krummacher, S.; Strogin, M.; Weng, S. L.; Wesner, D. Site-Specific Fragmentation of Small Molecules Following Soft-X-Ray Excitation. *Phys. Rev. Lett.* **1983**, *50*, 1038−1041.

(18) Nelson, M. C.; Murakami, J.; Anderson, S. L.; Hanson, D. M. Fragmentation of Acetone Following Excitation in the Region of the Oxygen K-Edge. *J. Chem. Phys.* **1987**, *86*, 4442−4445.

(19) Suzuki, I. H.; Saito, N. Energy Dependences of Fragment Ion Yields from Acetone Photoexcited in the C1s and O1s Transition Regions. *Chem. Phys.* **2000**, *253*, 351−359.

(20) Suzuki, I. H.; Saito, N. Cation Pair Formation from Acetone Following Monochromatic Soft X-ray Absorption. *Int. J. Mass Spectrom.* **2000**, *198*, 165−172.

(21) Koch, J. D.; Gronki, J.; Hanson, R. K. Measurements of Near-UV Absorption Spectra of Acetone and 3-Pentanone at High Temperatures. *J. Quant. Spectrosc. Radiat. Transfer* **2008**, *109*, 2037−2044.

(22) Fogleman, E. A.; Koizumi, H.; Kercher, J. P.; Sztaray, B.; Baer, T. Heats of Formation of the Acetyl Radical and Ion Obtained by Threshold Photoelectron Photoion Coincidence. *J. Phys. Chem. A* **2004**, *108*, 5288−5294.

(23) Rennie, E. E.; Boulanger, A. M.; Mayer, P. M.; Holland, D. M. P.; Shaw, D. A.; Cooper, L.; Shpinkova, L. G. A Photoelectron and TPEPICO Investigation of the Acetone Radical Cation. *J. Phys. Chem. A* **2006**, *110*, 8663−8675.

(24) Lepage, M.; Michaud, M.; Sanche, L. Low-Energy Electron-Energy-Loss Spectroscopy of Condensed Acetone: Electronic Transitions and Resonance-Enhanced Vibrational Excitations. *J. Chem. Phys.* **2000**, *112*, 6707−6715.

(25) Lepage, M.; Michaud, M.; Sanche, L. Low-Energy Electron Scattering Cross Section for the Production of CO Within Condensed Acetone. *J. Chem. Phys.* **2000**, *113*, 3602−3608.

(26) Kusunoki, I.; Sakashita, M.; Takaoka, T.; Range, H. Photodissociation and Desorption of Multilayer Acetone on a Si(100) Surface by 193 nm Laser Irradiation. *Surf. Sci.* **1996**, *357−358*, 693−697.

(27) Lightfoot, P. D.; Kirman, S. P.; Pilling, M. J. Photolysls of Acetone at 193.3 nm. *J. Phys. Chem.* **1988**, *92*, 4938−4946.

(28) Sekiguchi, T.; Sekiguchi, H. I.; Baba, Y. Site-Specific Fragmentation of Acetone Adsorbates on Si(100) in the Carbon 1s Absorption Edge. *Surf. Sci.* **2000**, *454−456*, 363−368.

(29) Trott, W. M.; Blais, N. C.; Walters, E. A. Molecular Beam Photoionization Study of Acetone and Acetone-d_6. *J. Chem. Phys.* **1978**, *69*, 3150−3158.

(30) Tamenori, Y.; Takahashi, O.; Yamashita, K.; Yamagushi, T.; Okada, K.; Tabayashi, K.; Gejo, T.; Honma, K. Hydrogen Bonding in Acetone Clusters Probed by Near-Edge X-ray Absorption Fine Structure Spectroscopy in the Carbon and Oxygen K-edge Regions. *J. Chem. Phys.* **2009**, *131*, 174311.

(31) Matsuda, Y.; Ohta, K.; Mikami, N.; Fujii, A. Infrared Spectroscopy for Acetone and its Dimer Based on Photoionization Detection with Tunable Coherent Vacuum-Ultraviolet Light. *Chem. Phys. Lett.* **2009**, *471*, 50−53.

(32) Guan, J.; Hu, Y.; Xie, M.; Bernstein, E. R. Weak Carbonyl-Methyl Intermolecular Interactions in Acetone Clusters Explored by IR plus VUV Spectroscopy. *Chem. Phys.* **2012**, *405*, 117−123.

(33) Rocco, M. L. M.; Weibel, D. E.; Roman, L. S.; Micaroni, L. Photon Stimulated Ion Desorption from Poly(3-methylthiophene) Following Sulphur K-shell Excitation. *Surf. Sci.* **2004**, *560*, 45−52.

(34) Mendoza, E.; Almeida, G. C.; Andrade, D. P. P.; Luna, H.; Wolff, W.; Rocco, M. L. M.; Boechat-Roberty, H. M. X-ray Photodesorption and Proton Destruction in Protoplanetary Discs: Pyrimidine. *Mon. Not. R. Astron. Soc.* **2013**, *433*, 3440−3452.

(35) Hitchcock, A. P.; Mancini, D. C. Gas Phase Core Excitation Database, available at http://unicorn.mcmaster.ca/corex/cedb-title.html.

(36) Ponciano, C. R.; Martinez, R.; Farenzena, L. S.; Iza, P.; Silveira, E. F.; Homem, M. G. P.; Brito, A. N.; Wien, K. Electronic Sputtering Produced by Fission Fragments on Condensed CO and CO_2. *J. Am. Soc. Mass. Spectrom.* **2006**, *17*, 1120−1128.
(37) Baba, Y. X-ray Induced Ion Desorption from Solid Surfaces. *Trends Vac. Sci. Technol.* **2002**, *5*, 45−74.
(38) Knotek, M. L. Stimulated Desorption. *Rep. Prog. Phys.* **1984**, *47*, 1499−1561.
(39) Ramaker, D. E.; Madey, T. E.; Kurtz, R. L. Secondary-Electron Effects in Photon-Stimulated Desorption. *Phys. Rev. B* **1988**, *38*, 2099−2111.
(40) Andrade, D. P. P.; Rocco, M. L. M.; Boechat-Roberty, H. M. X-ray Photodesorption from Methanol Ice. *Mon. Not. R. Astron. Soc.* **2010**, *409*, 1289−1296.
(41) Almeida, G. C.; Andrade, D. P. P.; Arantes, C.; Nazareth, A. M.; Boechat-Roberty, H. M.; Rocco, M. L. M. Desorption from Methanol and Ethanol Ices by High Energy Electrons: Relevance to Astrochemical Models. *J. Phys. Chem. C* **2012**, *116*, 25388−25394.
(42) Cottin, H.; Moore, M. H.; Bénilan, Y. Photodestruction of Relevant Interstellar Molecules in Ice Mixtures. *Astrophys. J.* **2003**, *590*, 874−881.
(43) Nuevo, M.; Milam, S. N.; Sandford, S. A.; Elsila, J. E.; Dworkin, J. P. Formation of Uracil from the Ultraviolet Photo-Irradiation of Pyrimidine in Pure H_2O Ices. *Astrobiology* **2009**, *9*, 683−695.
(44) Hudson, R. L.; Moore, M. H. Far-IR Spectral Changes Accompanying Proton Irradiation of Solids of Astrochemical Interest. *Radiat. Phys. Chem.* **1995**, *45*, 779−789.
(45) Heister, K.; Zharnikov, M.; Grunze, M.; Johansson, L. S. O.; Ulman, A. Characterization of X-ray Induced Damage in Alkanethiolate Monolayers by High-Resolution Photoelectron Spectroscopy. *Langmuir* **2001**, *17*, 8−11.
(46) Khriachtchev, L.; Pettersson, M.; Rasanen, M. On Self-Limitation of UV Photolysis in Rare-Gas Solids and Some of its Consequences for Matrix Studies. *Chem. Phys. Lett.* **1998**, *299*, 727−733.
(47) Pilling, S.; Andrade, D. P. P.; Nascimento, E. M.; Marinho, R. R. T.; Boechat-Roberty, H. M.; Coutinho, L. H.; Souza, G. G. B.; Castilho, R. B.; Cavasso-Filho, R. L. Photostability of Gas- and Solid-Phase Biomolecules Within Dense Molecular Clouds due to Soft X-rays. *Mon. Not. R. Astron. Soc.* **2011**, *411*, 2214−2222.
(48) Gorti, U.; Dullemond, C. P.; Hollenbach, D. Time Evolution of Viscous Circumstellar Disks due to Photoevaporation by Far-Ultraviolet, Extreme-Ultraviolet, and X-ray Radiation from the Central Star. *Astrophys. J.* **2009**, *705*, 1237−1251.
(49) Kastner, J. H.; Huenemoerder, D. P.; Schulz, S.; Canizares, C. R.; Weintraub, D. A. Evidence for accretion: High-Resolution X-Ray Spectroscopy of the Classical T Tauri Star TW Hydrae. *Astrophys. J.* **2002**, *567*, 434−440.
(50) Stelzer, B.; Schmitt, J. H. M. M. X-ray Emission from a Metal Depleted Accretion Shock onto the Classical T Tauri Star TW Hya. *Astron. Astrophys.* **2004**, *418*, 687−697.